

MICRODISPLACEMENT AND MICROVIBRATION SENSORS BASED ON SEMICONDUCTOR LASERS

**Vu Van Luc, P. G. Eliseev, M. A. Man'ko,
and M. V. Tsotsoriya**

Introduction

Semiconductor lasers and light-emitting diodes are widely used in various branches of science and engineering. They offer many significant advantages over other coherent-radiation sources: compactness, low cost, simplicity of pumping and modulation, compatibility with fiber optics, tunable frequency, reliability and long life, and extensive possibility of integrating optical systems. The advent of 1.3- and 1.55- μm lasers has initiated a new stage of their use in fiber-optics communication lines (FOCL). Advances in optical communication have increased, in turn, the interest in integration of optoelectronic systems capable of transmitting receiving and processing information at high speeds. In this sense, injection lasers are almost ideal light sources, since they can operate in various regimes: 1) as coherent light sources; 2) as amplifiers (of the traveling-wave or tuned type) and detectors; 3) as optical switches and modulators; 4) as negative-bias photodetectors. The versatility of injection lasers is one of their principal advantages. Advances in optical communication imposes new requirements on the properties of the lasers and stimulates further development of the technology, and investigations of various schemes and operating regimes of injection lasers.

Another most important application of semiconductor lasers is in optoelectronic sensors. Here, too, the advantages of semiconductor lasers have determined their possible use. Laser diodes are used in sensors for the measurement of a great variety of physical quantities, such as displacement and vibrations, temperature, pressure, velocity, acceleration, and electric and magnetic fields [1, 2]. All the sensor variants can be divided here into two types. In the first, the injection laser serves only as a source of light, while the sensitive element is, for example, an optic fiber (fiber-optics sensor). Progress in the development of this class of sensors is due both to the improvements of the sensitive element and to the development of light sources capable of meeting increased requirements (for example, with respect to line width or laser stability). In the second type of sensor the semiconductor laser acts both as a light source and as an element sensitive to the external action of various physical factors. These include sensors based on laser diodes with external optical feedback (OF) effected by introducing an external mirror that reflects the radiation back into the active medium of the laser. These sensors employ modulation of various laser properties due to modulation of the amplitude or phase of the FB. Introduction of optical feedback alters the spectral, noise, and threshold properties of the laser. Changing the threshold alters the output power as well as the voltage on the p-n junction. The sensitivity of the lasing regime to the amplitude and phase of the OF was investigated in detail in [3, 9]. The phase sensitivity was used in [10, 11] to measure microdisplacements and microvibrations of the external mirror. It was noted in [12] that it is possible to measure also a number of physical quantities whose variations can be converted into mechanical displacements, such as magnetic fields, acceleration, acoustic properties, etc. It was proposed in [13] to measure the angular velocity of a rotating disk by reflecting light from its dull surface back into the mirror (OF factor $\sim 10^{-5}$). The returning radiation is shifted in frequency by the Doppler effect, and its combination with the internal field produces beats in the diode. Measurement of the Doppler shift makes it possible to determine the disk speed. A displacement sensor and profilometer based on incoherent feedback of radiation reflected from a surface to a laser.

We have studied the sensitivity limit of a micromotion and microvibration sensor based on semiconductor lasers, and have constructed several variants of such sensors.

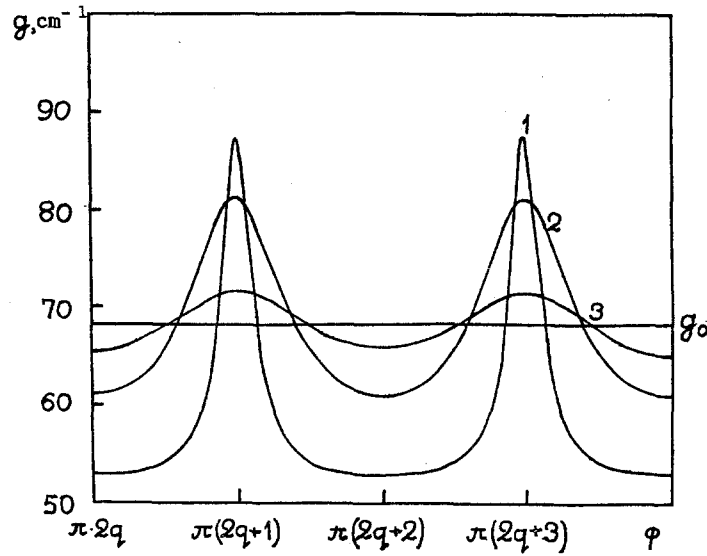


Fig. 1. Threshold gain g in external cavity vs. the feedback phase $\phi = 4\pi L/\lambda$ at various values of the mirror reflection coefficient R . The remaining parameters are $\alpha = 20 \text{ cm}^{-1}$, $l = 250 \text{ }\mu\text{m}$, $n^* = 1.6$, $\lambda = 1.3 \text{ }\mu\text{m}$, $\chi = 0.7$, $R = 1$ (1), 0.1 (3), $r = 0.3$.

1. Estimate of Sensitivity Limit of a Sensor for Microdisplacements and Microvibrations

The operating principle of such a sensor, as already noted, is based on the sensitivity of laser operation in an external compound cavity to the position of the external reflecting surface (mirror), which is optically coupled to a laser diode. A change of the external-mirror position (of the feedback) alters the threshold lasing current and hence, at a given pump current, the output power and the diode voltage. By measuring the increment of the output power or of the voltage one can assess the change of the external-mirror position. Let us examine on the basis of a three-mirror compound cavity, in the single-frequency approximation, the signal/noise ratio (SNR) and the maximum sensitivity (detection ability) of a microdisplacement sensor in both registration regimes — in optical registration (the signal is the variation of the radiation power) and in the optoelectronic regime (the signal is the change of the voltage on a diode).

The threshold condition in an external compound cavity can be written in the form [15]:

$$e^{(g-\alpha)l} = \frac{1 + \sqrt{rR} e^{-4\pi i L/\lambda}}{\sqrt{r} e^{-4\pi i n^* l/\lambda} (\sqrt{r} + \chi \sqrt{R} e^{-4\pi i L/\lambda})} \quad (1)$$

where g is the threshold value of the gain, α the nonresonant-loss exponent, l the length of the laser diode, L the length of the external part of the compound cavity, n^* the group refractive index in the active region, λ the radiation wavelength in vacuum, r the power reflection coefficient of the end face of the diode, R the reflection coefficient of the external mirror, $\chi = R + (1 - r)\kappa$, and κ is the power-input coefficient of the radiation reflected back to the active region. Equation (1) leads to an expression for the lasing frequency (frequencies) and for the increment Δg of the threshold gain in the external cavity (compared with the threshold $g_0 = \alpha + \frac{1}{l} \ln \frac{1}{r}$ of the diode itself):

$$\omega_p - \omega = \frac{c}{2n^* l} \text{Arctg} \frac{(\chi - r) \sqrt{R} \cdot \sin \phi}{(1 + R \chi) \sqrt{r} + (\chi + r) \sqrt{R} \cdot \cos \phi} \quad (2')$$

$$\Delta g \equiv g - g_0 = \frac{1}{l} \ln \left\{ \sqrt{r} \cdot \frac{(1 + \chi R) \sqrt{r} \cdot \cos \phi_1 + r \sqrt{R} \cdot \cos(\phi_1 - \phi) + \chi \sqrt{R} \cdot \cos(\phi_1 + \phi)}{r + \chi^2 \cdot R + 2\chi \sqrt{Rr} \cdot \cos \phi} \right\} \quad (2'')$$

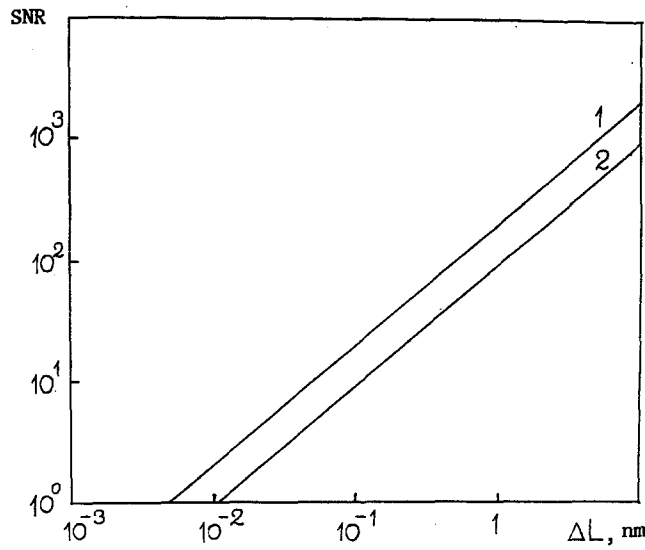


Fig. 2. Signal/noise ratio vs. external-mirror displacement ΔL in the optical-registration (1) and optoelectronic (2) regimes. The parameters employed are $l = 250 \mu\text{m}$, $\alpha = 20 \text{ cm}^{-1}$, $\lambda = 1.3 \mu\text{m}$, $r = 0.3$, $R = 1$, $\kappa = 0.3$, $mkT/e = 30\text{mV}$, $\eta = 0.2 \text{ mW/mA}$, $\beta = 2 \text{ cm}^{-1}\cdot\text{mA}^{-1}$, $\delta P = 0.05 \mu\text{W}$, $\delta V = 0.5 \mu\text{V}$.

where $\omega_p = \pi p(c/n^*l)$, p is the index of the laser-diode modes and is an integer, ω is the lasing frequency in the external cavity $\phi_1 = (4\pi/\lambda)n^*l$, and $\phi_1 = (4\pi/\lambda)L$ is the phase of the external feedback.

For low values of the external-mirror reflection coefficient, $R \rightarrow 0$, we obtain

$$\omega_p - \omega \approx \frac{c}{2n^*l} \kappa(1-r) \sqrt{\frac{R}{r}} \cdot \sin \phi \rightarrow 0 \quad (3')$$

$$\Delta g \approx -\frac{1}{l} \kappa(1-r) \sqrt{\frac{R}{r}} \cdot \cos \phi \quad (3'')$$

Figure 1 shows the dependence of the threshold gain g in the external cavity on the FB phase ϕ at various values of the external-mirror reflection coefficient R .

Obviously, optimal operation of the sensor requires a suitable choice of the working point (the initial position of the external mirror) on the linear section, where the response of different laser characteristics to a change of the laser position is a maximum. We choose an initial mirror position at which the lasing threshold in the external cavity is equal to the diode's own threshold; the corresponding working point is on the linear section (see Fig. 1), and the change of the threshold gain is determined by Eq. (2) (the FB phase is in this case $\phi = \phi_0 + (4\pi/\lambda)\Delta L$, where ΔL is the displacement of the external mirror from the initial position and ϕ_0 is determined from the equation $\Delta g = 0$).

The threshold change due to introduction of external optical feedback alters the radiation power and the voltage on the diode. Recognizing that the injection current below the threshold is $I \sim \exp(eV/mkT)$ and exceeds above the threshold the saturation voltage on a p-n junction [16], and assuming linear relations between the gain and the current, $g = \beta I$, and between the radiation power P and the current, $P = \eta(I - I_s)$, we obtain the following expressions for the changes of the power and voltage:

$$\Delta P = -\frac{\eta}{\beta} \Delta g; \quad (4')$$

$$\Delta V = \frac{mkT}{e} \ln \left(1 + \frac{\Delta g}{g_0} \right). \quad (4'')$$

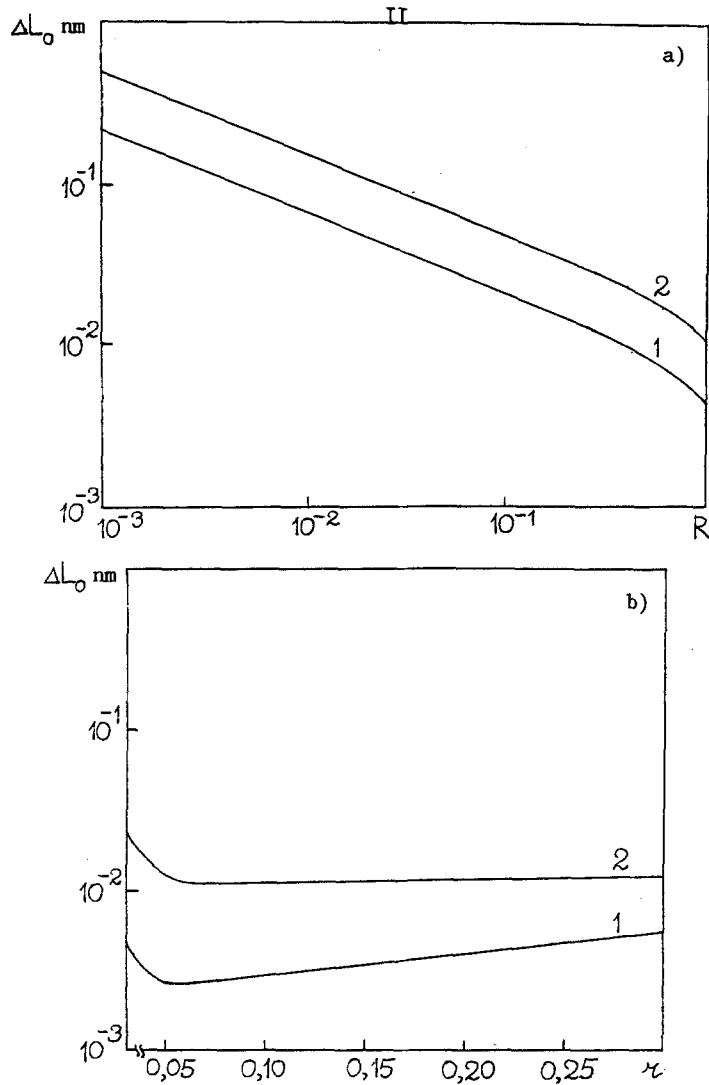


Fig. 3. Detecting ability ΔL_0 vs. the reflection coefficients of the external mirror (a) and the front face of the diode (b) in the optical-recording (1) and the optoelectronic (2) regimes. The values of the employed parameters are the same as in Fig. 2.

where η is the differential effectiveness of the watt-ampere characteristic, kT is the temperature of the laser diode, and m is called the “non-ideality” coefficient of the current-voltage characteristic of the laser.

Equations (4) show the dependences of the recorded signal (of the increase of power or voltage) on the displacement ΔL . In sensors for microdisplacements and microvibrations, however, an important property is not only the value of the signal, but also the signal/noise ratio (SNR) and the detection ability (which we define as the external-mirror displacement ΔL_0 corresponding to unity SNR).

Of basic interest for sensors is the low-temperature region (to 100 kHz). Predominant in injection lasers for this region are the so-called $1/f$ (f is the frequency) power and voltage noises due to various causes. The spectral densities of these noises are $G_p(f) = A/f$ and $G_v(f) = B(f)$. The characteristic values of the coefficients A and B are $A' \sim 10^{-15} \text{ W}^2$ [17]; $B' \sim 10^{-13} \text{ V}^2$ [18]. Addition of external feedback, however, raises the noise level; in the feedback region of interest for sensors (0.1-10%) the noise increment does not exceed 20 dB [20]. For a laser with an external cavity one can therefore use the estimates $A' \sim 10^{-13} \text{ W}^2$; $B' \sim 10^{-11} \text{ V}^2$.

The errors in the measurement of the power and voltage are connected with the corresponding spectral densities of the noises by the expression

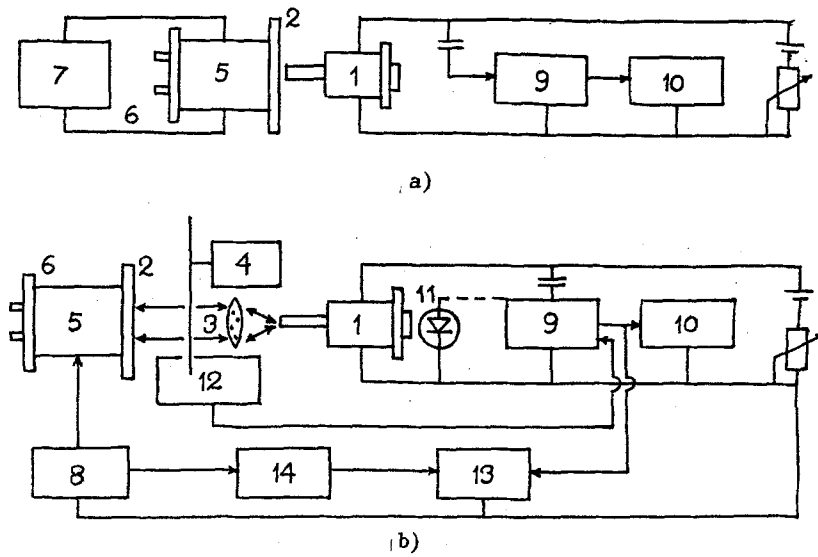


Fig. 4. Block diagram of the experimental setup for the investigation of the possibility of using the commercial ILPN-202 laser as a microdisplacement sensor: a) system for plotting the dependence of the optoelectronic signal on the laser pump current; b) system for plotting the signal amplitude vs. the mirror displacement. 1) Laser diode; 2) mirror; 3) micro-objective; 4) mechanical chopper; 5) piezoceramic base; 6) micrometric stage; 7) pulsed-voltage generator; 8) high-voltage dc source; 9) electronic amplifier with lock-in detector; 10) oscilloscope; 11) photodiode; 12) reference-signal block for lock-in detector; 13) automatic x-y plotter; 14) voltage divider.

$$\delta P = \left[\int_{f_1}^{f_2} (A'/f) df \right]^{1/2}; \quad (5')$$

$$\delta V = \left[\int_{f_1}^{f_2} (B'/f) df \right]^{1/2} \quad (5'')$$

where f_1 and f_2 are the lower and upper frequencies defining the signal-recording band. In a selective regime using, for example, a frequency 1 kHz and a bandwidth 20 Hz the estimated errors are $\delta P \sim 0.05 \mu W$; $\delta V \sim 0.5 \mu V$.

The signal/noise ratio can be expressed in the form $(SNR)_P = \Delta P/2\delta P$; $(SNR)_V = \Delta V/2\delta V$ (the reason for the factor 2 in the denominator is that differences of powers or voltages are measured in two states of the external cavity).

The dependences of the signal/noise ratio on the displacement ΔL of the external mirror in both recording regimes at $\delta P = 0.05 \mu W$ and $\delta V = 0.5 \mu V$ are shown in Fig. 2. The detection ability ΔL_0 of the sensor is $5 \cdot 10^{-3} \text{ nm}$ in optical registration regime and 0.012 nm in the optoelectronic regime.

The detection abilities are given by the expressions

$$\Delta L_0^P \approx \frac{\lambda}{2\pi} \frac{2\delta P \cdot \beta}{\eta} \frac{r(1-R\chi)}{(\chi-r)\sqrt{4rR - (\chi+r)^2 R^2}}; \quad (6')$$

$$\Delta L_0^V \approx \frac{\lambda}{2\pi} \frac{2\delta V \cdot e}{mkT} \frac{r(1-R\chi)(\alpha l + \ln 1/r)}{(\chi-r)\sqrt{4rR - (\chi+r)^2 R^2}} \quad (6'')$$

Figures 3a and 3b show respectively the calculated dependences of the detection ability on the reflection coefficients R and r of the external mirror and r of the front (facing the external mirror) face of the diode, respectively. Optimization calls bleaching of the front face.

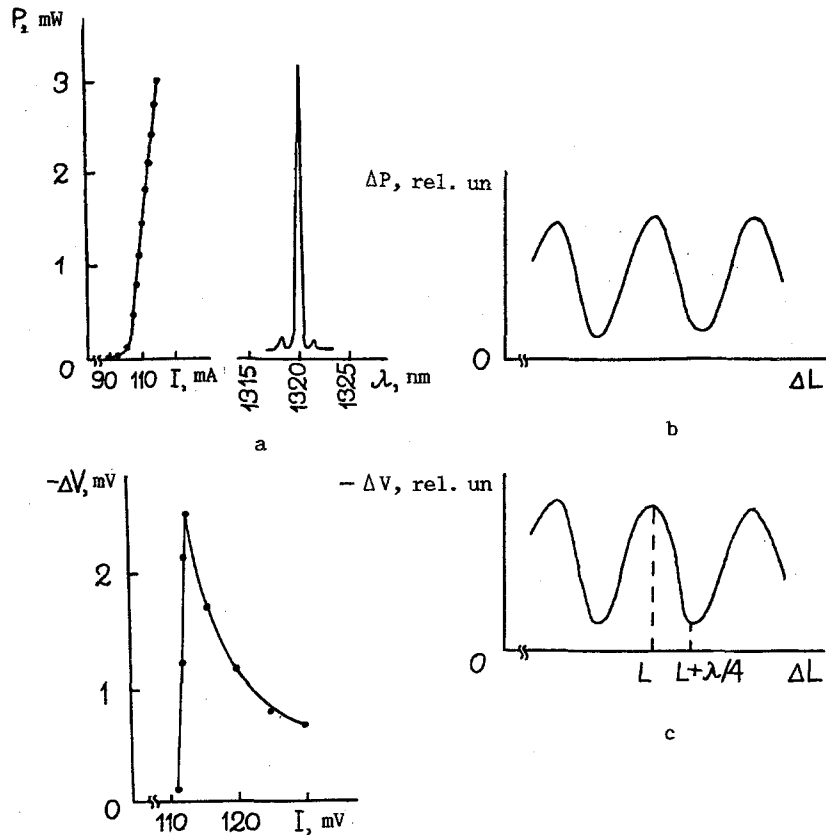


Fig. 5. a) Watt-ampere and spectral characteristics of the employed laser-diode sample; b) dependence of the optoelectronic signal ΔV on the laser pump current; c, d) dependences of the optical signal ΔP (c) and of the optoelectronic signal (d) on the displacement ΔL of the mirror ΔL at fixed values of the pump current.

The sensor sensitivity can be raised by using various stabilization systems that lower the noise in the system to the level typical of the laser in the free-running regime (without optical feedback). In real sensors, on the other hand, the above estimate of the detection ability can be made worse by noise from the photodiode (with a level usually lower than the noise level of the laser itself), from the pump and recording systems, from additional parasitic reflection from the matching optical systems, from additional radiation modes (the analysis above was made in the single-mode approximation), and from the "phasing properties" of the reflecting surface.

In the optimal regime, therefore, a semiconductor-laser microdisplacement sensor is expected to have a detecting ability at a $\sim 10^{-2}$ nm level.

2. Microdisplacement Sensor Based on the Serially Manufactured ILPN-202 Laser Diode

Practical applications require production of microdisplacement and microvibration sensors based on semiconductor injection lasers in a design that is most convenient in use. The commercial serially manufactured ILPN-202 laser diode can be used as a sensor for sub-micron displacements. Such a sensor consists of the laser proper and a probed mirror surface parallel and close enough to the exit window of the laser housing (it is assumed that the length of the external optical link does not exceed the coherence length of the radiation). A block diagram of the experimental setup is shown in Fig. 4. Radiation at a wavelength $1.3 \mu\text{m}$ from the commercial laser diode ILNP-202 (1), fed with direct current, was directed to the external flat mirror 2 having a reflection coefficient 70% either directly (Fig. 4a; the distance between the fiber output of the laser housing

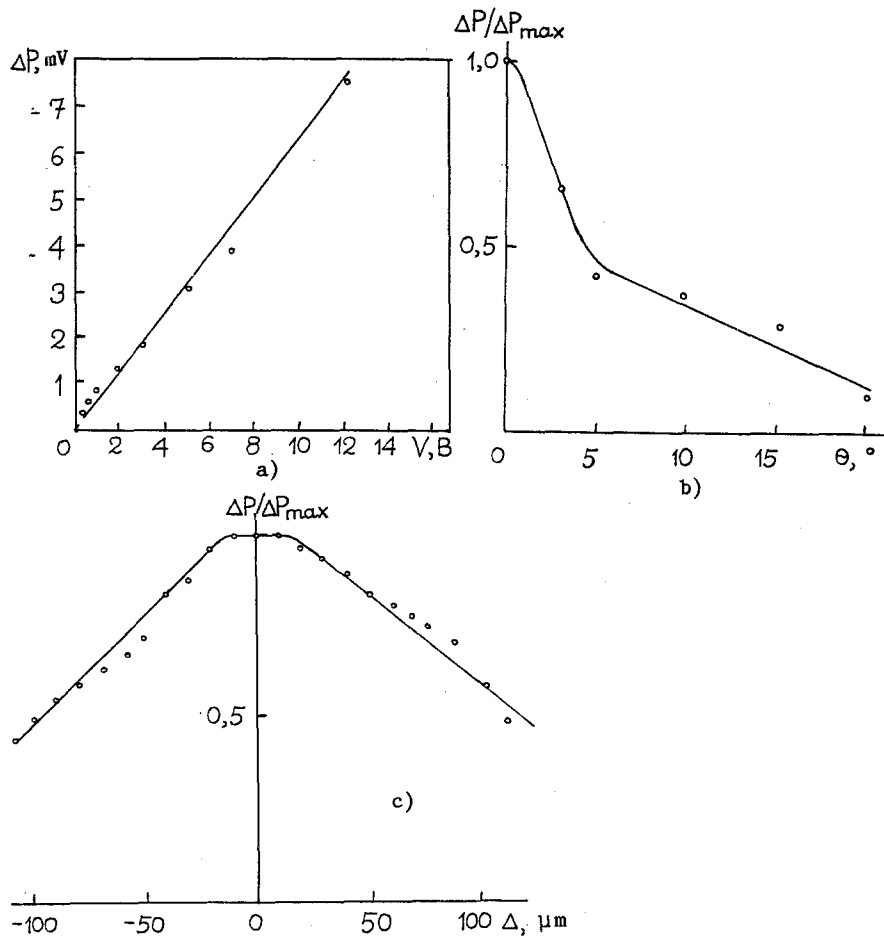


Fig. 6. a) Dependence of the optical signal ΔP on the amplitude of the voltage applied to the ceramic; b, c) dependences of the normalized optical signal on the longitudinal displacement (b) and on the rotation angle of laser cartridge (c).

and the mirror was $25 \mu\text{m}$), or through micro-objective 3 and a mechanical chopper 4 (Fig. 4b; in this case the mirror could be moved 10 cm away without substantial loss to the optoelectronic-signal amplitude. Mirror 2 was mounted on piezo-ceramic base 5 secured to micrometric stage 6. In the system of Fig. 4a, we applied a pulsed voltage of amplitude up to 50 V, which displaced the mirror by not less than $\lambda/4$. In the system of Fig. 4b, the mirror was displaced by applying dc voltage (0-600 V) to the piezoceramic base. The electric response ΔV to the external optical feedback (i. e., the optoelectronic signal produced by the longitudinal displacement of the mirror) was enhanced by amplifier 9 and observed on oscilloscope 10. The system of Fig. 4 measured the optoelectronic as well as the signal picked off by photodiode 11 from the second laser-exit lightguide output. The electronic amplifier 9 operated in the lock-in detection regime, with the frequency of the reference signal likewise set by the mechanical chopper 4. The detector was the oscilloscope 10 or the x-y automatic plotter 13 whose horizontal coordinate received through divider 14 the voltage from the power supply of the piezoceramic base.

The characteristics of the sample employed are shown in Fig. 5a. The threshold current was 102 mA and the lasing wavelength was 1320 nm. The laser watt-ampere characteristic was linear, and a single-frequency spectrum was preserved up to 150% threshold. Figure 5b shows the dependence of the optoelectronic signal on the pump current at the optimum tuning corresponding to a longitudinal displacement of the mirror by $\lambda/4$. The signal reaches its maximum 2.5 mV at the lasing threshold, after which it decreases with increase of current. Figure 5c shows plots of the optoelectronic and optical signals ΔV and ΔP , respectively, obtained with the scheme of Fig. 4b, against the longitudinal mirror displacement ΔL at a fixed value of the current. These plots, as expected, are periodic with a period $\lambda/2$. The linear section of the plot of ΔV extends to a mirror displacement $\Delta L \approx 230 \text{ nm}$, and the corresponding optoelectronic signal is $\Delta V = 2.3 \text{ mV}$ (at the lasing threshold). Consequently,

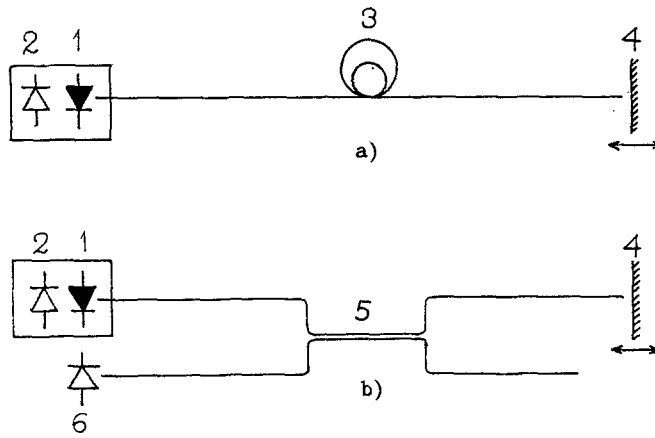


Fig. 7

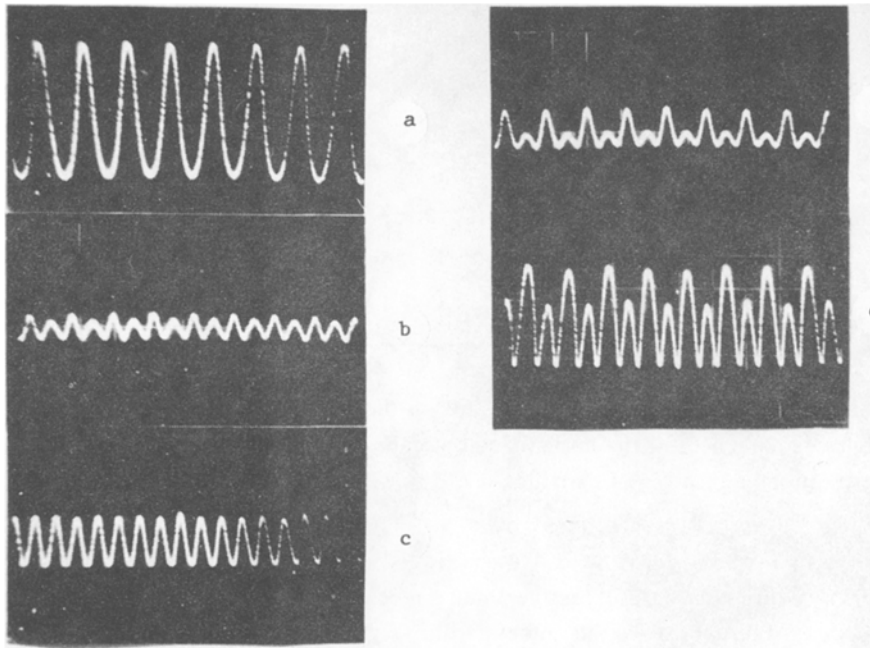


Fig. 8

Fig. 7. Various signal-registration schemes: a) direct sounding; b) using a fiber directional coupler. 1) Laser diode; 2) control photodiode; 3) lightguide channel; 4) probed surface (mirror); 5) fiber directional coupler; 6) external photodiode.

Fig. 8. Waveforms of photoresponse to mirror vibration. The working point is located: a) on the linear section; b, c) in the extreme; d, e) on the transition sections of the sinusoid-like static characteristic.

the sensitivity of the sensor to small displacements was $\Delta V/\Delta L \approx 10 \text{ mV}/\mu\text{m}$. Proper stabilization of the laser operating regime permits submicron displacements to be measured. For example, if the voltage noise permits a $10\text{-}\mu\text{V}$ variation to be recorded, displacements $\sim 10^{-3} \mu\text{m}$ can be measured.

In contrast to interferometric sensors based on gas lasers, in our present case the construction is substantially simpler, more compact and economical, as well as more reliable. The special requirements for this sensor to be serviceable reduce to the following: 1) The probed plane must be specular and perpendicular to the laser-beam axis; 2) the gap between the tip of the laser fiber lead and the probed plane (in the absence of a collimator) must be in the $5\text{-}50 \mu\text{m}$ interval; 3) the pump current

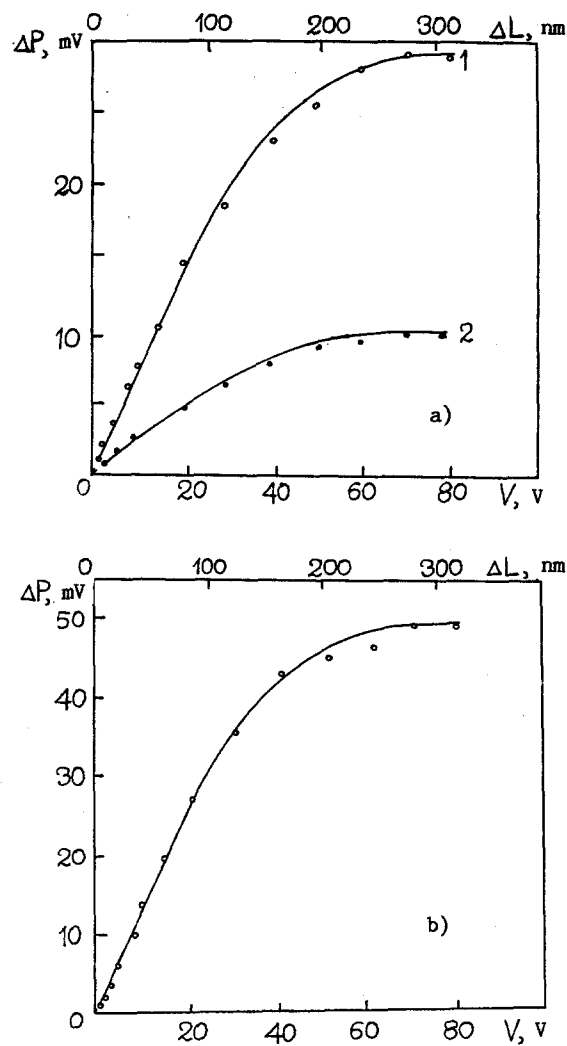


Fig. 9. Sinusoidal photoresponse vs. amplitude of the voltage on the ceramic and vs. the vibration amplitude; a) direct probing scheme, fiber lead length $L = 1$ m (1) and $L = 300$ m (2); b) in a system with fiber directional coupler.

must be maintained at the threshold level, i.e., it is advantageous to stabilize the current and temperature of the laser diode (since the threshold is temperature-dependent).

Thus, the commercial ILPN-202 laser, without change of construction and even without additional optical accessories can serve as a sensitive microdisplacement sensor. This is of particular practical importance, since development of semiconductor injection lasers for similar sensor was frequently hindered by construction features of ordinary commercial laser diodes.

3. Microvibration Pickup Based on a Laser Cartridge

The microvibration sensor used was a laser cartridge emitting at $0.85 \mu\text{m}$. The laser cartridge contained a laser diode, an objective, and a control photodiode to record the radiation from the rear face of the diode. The objective focused the laser radiation onto a mirror secured to a piezoceramic base. A sinusoidal 15-kHz voltage was applied to the ceramic. The piezoelectric conversion coefficient was 0.8 nm/V . The threshold current of the employed GaAlAs/GaAs laser sample was 120 mA, and the working-current range was 140-160 mA (in this range, the response to mirror vibrations recorded by the control photodiode was a maximum and almost constant).

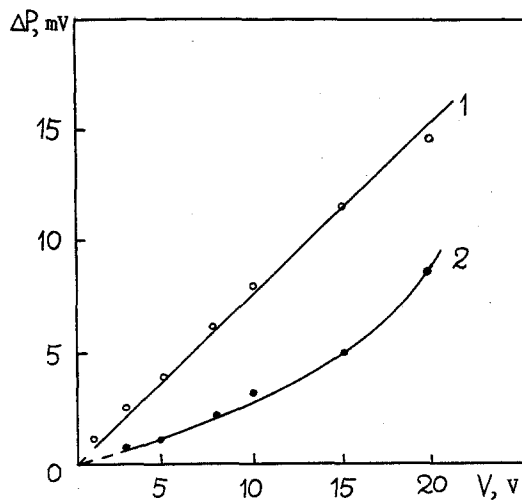


Fig. 10. Photoresponse vs. the amplitude of the voltage on the ceramic in the direct probing scheme. The working point is: 1) on the linear section; 2) at the extremum of the static characteristic.

Figure 6a shows the photoresponse as a function of the amplitude of the voltage on the ceramic for the optimal (7 mm) distance between the mirror and the output window of the laser cartridge. The detection ability was ~ 0.4 nm.

An important problem in the practical application of the sensors is that of the displacement tolerances and of rotation away from the optimal position. A plot of the normalized optical signal vs. the longitudinal displacement of a laser cartridge from optimal position is shown in Fig. 6b. The displacement tolerance (i. e., the displacement at which the signal is decreased by one-half) is 100 μm . Figure 6c shows the dependence of the normalized optical signal on the cartridge rotation angle. The rotation tolerance is 4° .

The foregoing characteristics of a microvibration sensor based on a laser cartridge are fully acceptable for various practical applications.

4. Microvibration Sensor Based on the LMF-1300 Semiconductor Laser Module

Semiconductor laser modules are usually developed for information transmission over fiberoptics communication lines [20-21]. We used an LMF-1300 single-mode 1.3- μm laser module in various microvibration sensor schemes. The module contained an InGaAsP/InP heterolaser, a control photodiode to record radiation from the rear face of the laser diode, and a single-mode fiber output lead. The surface whose displacement (vibration) was measured was a planar mirror secured to a piezoceramic base. A sinusoidal or dc voltage was applied to the piezoceramic. Application of 80 V produced displaced the mirror by $\lambda/4$. The experiments were performed both by direct sounding (Fig. 7a) and by using a directional coupler (Fig. 7b; the coupler ratio is 1:1.2 and its loss is < 1 dB). The laser response to displacement of the mirror was recorded with a controllable photodiode in case a) and with an additional external diode in case b) (Fig. 7b). The signal could be recorded also by measuring the voltage on the diode. The distance from the end face of the lightguide to the mirror was 10-60 μm .

Note that the output end of the fiber forms together with the mirror a supplementary Fabry-Perot interferometer having a separate sensitivity to displacements; it is therefore possible to record displacements (vibrations) of the mirror with the aid of a supplementary photoreceiver using only the reflected light (Fig. 7b), without resorting to feedback. This is the more traditional interferometry scheme, which was found to have a higher sensitivity than the direct sounding scheme.

In direct-sounding experiments, the pump current of the module was located in the immediate vicinity of the threshold (in this case the signal of the control photodiode is a maximum). In the static regime with displacements of the mirror (a dc voltage was applied to the ceramic) the photoresponse depended on the voltage applied to the ceramic, with a certain positive background, while in the dynamic regime (a sinusoidal voltage applied to the ceramic) the form of the response was determined by the location of the working point on the static characteristic. For example, with the working point on the linear section of

the sinusoid, the photodiode response to mirror vibrations of small amplitude ($< \lambda/4$) duplicates the form of the voltage on the ceramic (Fig. 8a) whereas if the working point is located at an extremum of sinusoid-like static characteristic we get a response at double the mirror-vibration frequency (Figs. 8b, c). The photoresponse forms shown in Figs. 8d, e correspond to a transitional working point. Figure 9a shows a sinusoidal response as a function of the amplitude of the voltage on the ceramic (curve 1; by amplitude we mean here the distance between the extremal points). The frequency of the sinusoidal voltage on the ceramic was 500 Hz; the picture is qualitatively the same for other frequencies, from 100 Hz to 100 kHz. It is seen from the figure that it is possible to record mirror vibrations of amplitude 4 nm (corresponding to a voltage amplitude 1 V). The figure shows also the same dependence for a fiber lead from the module 300 m long (curve 2). The picture is in principle unchanged, while the decrease of the signal is due to attenuation of the light as it passes through the fiber. One can observe in this case vibrations 12 nm in amplitude. It is thus possible to use similar sensors in long-distance schemes, where the measurement block and the investigated object can be separated in space. The detecting ability of a sensor in a scheme with a fiber directional coupler amounted to ≈ 1.5 nm (Fig. 9b).

The response of the laser output power to the periodic displacements it produces in the mirror have already been investigated earlier [5]. To interpret this effect it was assumed that the frequency of the radiation reflected from the mirror is, on account of the Doppler effect, different from that of the laser, so that beats of the pump current and output power are produced. In our opinion, however, the predominant effect is just the Q-switching of the cavity as a function of the length of the external feedback. It is confirmed by the fact that the maximum photoresponse in the static regime of the mirror displacement was (29 ± 2) mV for an output-fiber length $L = 1$ m and (9 ± 2) mV for $L = 300$ m, i.e., equal within the limits of error to the maximum amplitude of the dynamic photoresponse (Fig. 9a). One more proof is that, depending on the position of the working point on the sinusoidal static characteristic at low ceramic-voltage amplitude the photoresponse was either linear in this amplitude (the working point is on the linear section of the sinusoid) or quadratic (working point at an extremum of the static characteristic), as shown in Fig. 10.

The error in the measurement of the vibration amplitude is determined by the sum of errors due to the recording system and to the sensor (laser + mirror) itself. The regular relative error of the electric recording system did not exceed 10%. Obviously, the relative error in the measurement of the vibration amplitude is also the same on the linear section. As for the error due to the sensor itself, it is equal to the detection ability (the vibration amplitude at unity signal/noise ratio) and amounts to 4 nm in the direct sounding scheme and to 1.5 nm in the scheme with a fiber directional coupler.

It is known that the sensor operation requires a thorough stabilization of the laser regime and of the external-feedback length. In our case, the influence of slow changes of the ambient temperature become particularly strongly manifested owing to the presence of fiber. A temperature drift in the range $\Delta T = \pm 0.1^\circ\text{C}$ produces in the fiber an optical-path drift $\pm(\alpha_T \cdot n \cdot L \cdot \Delta T) = \pm(0.5 \cdot 10^{-6} \text{ deg}^{-1} \times 1.5 \times 1 \text{ m} \times 0.1^\circ\text{C}) = \pm 75$ nm (α_T is the linear temperature-expansion coefficient). This causes the working point, and with it the shape of the photoresponse, to drift in time, as was indeed observed in practice. No obstacles to the measurement resulted, however; the end of the fiber was secured to the ceramic base to which the dc voltage was applied. If the shape of the signal was altered by variation of the voltage on the ceramic, it was possible to return to the linear working point and carry out the measurement.

The LMF-1300 single-mode laser module can thus be used as a microvibration sensor capable of detecting vibration amplitudes 4 nm by direct sounding and 1.5 nm when a single-mode fiber directional coupler is used. A remote sensor (fiber output lead 300 m) was produced with a 12 nm detecting ability.

CONCLUSION

The above analysis of a microvibration sensor based on a semiconductor laser has shown that in the optimal operating regime one can expect a detection ability of $\sim 10^{-2}$ nm.

It is preferable to record an optical signal (change of radiation power) than an optoelectronic one (change diode voltage).

Several sensor variants were constructed: with an ILPN-202 commercial laser diode, with a laser cartridge, and with the LMF-1300 single-mode laser module. Since real sensors contain additional noise sources (pumping- and recording-system noise, fluctuations due to parasitic reflection, etc.), the sensitivity limit could not be reached. The detection ability ranges, depending on the scheme employed, from fraction of a nanometer to several nanometers, but is perfectly acceptable for many practical applications.

LITERATURE CITED

1. V. I. Burusin, A. S. Semenov, and N. P. Udalov, "Optical and fiber-optics sensors," *Kvantovaya Elektron. (Moscow)*, **12**, 901-944 (1985).
2. B. A. Karasyuk, S. G. Semenov, A. G. Sheremet'ev, et al., *Fiber Optics Sensors [in Russian]*, Mashinostroenie, Moscow (1990).
3. W. J. Burke, M. Ettenberg, and H. Kresel, "Optical feedback effects in cw injection lasers," *Appl. Opt.*, **17**, No. 14, 2233 (1978).
4. Y. Mitsuhashi, T. Morikawa, K. Sakurai, et al., "Self-coupled optical pickup," *Optics Commun.*, **17**, No. 1, 95 (1976).
5. V. V. Dementienko, É. É. Godik, Yu. V. Gulyaev, et al., "Coherent registration of radiation with an injection laser," *Pis'ma Zh. Tekh. Fiz.*, **5**, 1349 (1979).
6. Y. Mitsuhashi, J. Shimada, and S. Mitsutsuka, "Voltage change across the self-coupled semiconductor laser," *IEEE J. Quantum Electron.*, **QE-17**, No. 7, 1216-1225 (1981).
7. Vu Van Lyk, P. G. Eliseev, M. A. Man'ko, et al., "Optoelectronic reading with the aid of an injection laser," *Kvantovaya Elektron. (Moscow)*, **9**, 1825 (1982).
8. Vu Van Lyk, P. G. Eliseev, M. A. Man'ko, et al., "Saturation of injection-contact voltage in a laser diode and the negative photo-emf phenomenon," *Trudy FIAN*, **166**, 174 (1986).
9. Vu Van Lyk, P. G. Eliseev, M. A. Man'ko, et al., "Electric response in InGaAsP/InP heterolasers," *Kvantovaya Elektron. (Moscow)*, **15**, 2227 (1988).
10. Vu Van Lyk, P. G. Eliseev, M. A. Man'ko, et al., "Microdisplacement sensors based on the ILPN-202 laser diode," *Kratk. Soobshch. Fiz. FIAN*, No.4, 42 (1988).
11. Vu Van Lyk, P. G. Eliseev, M. A. Man'ko, et al., "Optoelectronic microdisplacement sensor using an LMF-1300 semiconductor module," *All-Union Conf. on Problems of Optical Memory*, Telavi, 1990; Abstracts, Moscow (1990), pp. 246-247
12. R. O. Miles, A. Dandridge, A. B. Tveten, et al., "An external cavity diode laser sensor," *J. Lightwave Technol.*, **1**, 81 (1983)
13. S. Shinohara, A. Mochizuki, H. Yosida, et al., "Laser Doppler velocimeter using the self-mixing effect of semiconductor laser diode," *Appl. Opt.*, **25**, No. 9, 1417 (1986).
14. V. N. Morozov, P. V. Myasnikov, and S. E. Solodov, "Precision measurement of the surface quality of parts with the aid of optoelectronic sensors based on semiconductor lasers," *FIAN Preprint No. 134*, Moscow (1989).
15. J. H. Osmundsen and N. Gade, "Influence of optical feedback on laser-frequency spectrum and threshold conditions," *IEEE J. Quantum Electron.*, **QE-19**, No. 3, 465 (1983).
16. P. G. Eliseev, *Introduction to Physics of Injection Lasers [in Russian]*, Nauka, Moscow (1983).
17. R. J. Fronen and L. K. J. Vandamme, "Low-frequency intensity noise in semiconductor lasers," *IEEE J. Quantum Electron.*, **QE-24**, No. 5, 724 (1988).
18. V. M. Gilekonov, Yu. M. Mironov, and Ya. I. Khanin, "Relationship between low-frequency fluctuations of the radiation intensity and voltage fluctuations in semiconductor lasers," *Kvantovaya Elektron. (Moscow)*, **15**, 1999 (1988).
19. O. Hirota and Y. Suematsu, "Noise properties of injection lasers due to reflected waves," *IEEE J. Quantum Electron.*, **QE-15**, 142 (1979).
20. Bui Zui, Vu Van Lyk, P. G. Eliseev, et al., "Semiconductor laser emitters for single-mode information-transfer systems," *Trudy FIAN*, **189**, 133 (1989).
21. Vu Van Lyk, P. G. Eliseev, M. A. Man'ko, et al., "Single-mode transmission modules for fiber-optics lines, operating at wavelengths 1.3 mm and 1.55 mm," *FIAN Preprint No. 137*, Moscow (1989).